

Article

Comparative Study Involving Effect of Curing Regime on Elastic Modulus of Geopolymer Concrete

Peiman Azarsa  and Rishi Gupta * 

Department of Civil Engineering, University of Victoria, Victoria, BC V8P 5C2, Canada; azarsap@uvic.ca

* Correspondence: guptar@uvic.ca

Received: 27 March 2020; Accepted: 27 May 2020; Published: 30 May 2020



Abstract: Geopolymer Concrete (GPC) as a cement-less construction material has attracted worldwide attention due to its lower carbon footprint. There are numerous studies reported on GPC made using different by-products including fly-ash. However, since the use of bottom-ash is comparatively limited, making potassium-based GPC using this waste can be an alternative to Portland Cement Concrete (PCC). In this study, two methods of accelerated curing were used to determine the influence of elevated temperature on the compressive strength of GPC, composed of 50% bottom-ash and 50% fly-ash. GPC specimens were cured using various temperatures including ambient, 30 °C, 45 °C, 60 °C, and 80 °C for 24 h, all followed by 28 days of ambient curing. The highest compressive strength was obtained with steam curing at a temperature of 80 °C for a duration of 24 h. It is of great significance to evaluate elastic modulus of the concrete mixture so that the short-term rigidity of structures subjected to elongation, bending, or compression can be predicted. In this study, a longitudinal Resonant Frequency Test (RFT) as a non-destructive test (NDT) was used to calculate the elastic modulus of both GPC and a comparative PCC mix. Based on the results, PCC had higher resonant frequency (by about 1000 Hz) compared to GPC. A review of empirical models for predicting GPC's elastic modulus showed that all of the predicted elastic modulus values were lower than experimental values.

Keywords: geopolymer concrete; curing regime; resonant frequency; elastic modulus; predictive models

1. Introduction

One of the main environmental issues associated with the production of cement is Green House Gas (GHG) emissions to the atmosphere, as well as the consumption of natural resources. It is estimated that one ton of cement production needs about 1.5 tons of natural resources and emits about one ton of carbon dioxide (CO₂) into the air [1–3]. On the other hand, about 112 million tons of fly-ash as waste material is produced annually in the world [4]. So, the use of fly-ash in the concrete mixture can produce positive environmental, economic, and product benefits [5]. However, about 80% of the unburned material or fly-ash is entrained in the flue gas when pulverized coal is burned in a dry condition. The remaining 20% of the ash is dry bottom-ash that has similar chemical properties to fly-ash, consisting of silica and alumina. In the United States in 2017, 38.2 million tons of fly-ash and 9.7 million tons of bottom-ash were generated [6]. However, the use of bottom-ash is relatively limited, thus dealing with this industrial material is posing to be one of the most significant challenges in recent years. This is why a combination of bottom-ash and fly-ash was used to develop a cement-less concrete mix by the authors in this study. To the authors' knowledge, limited studies have been done that deal with this combination [7–9].

Geopolymer concrete (GPC) is a type of cement-less concrete that is produced using alumino-silicate material such as fly-ash and has the potential to decrease the significant carbon footprint associated with the production of cement. GPC is an alumino-silicate polymer (inorganic) which is made

using geological origin materials or industrial materials including fly-ash, slag, metakaolin, etc. The polymerization process involves a substantial chemical reaction of alumino-silicate species under alkaline conditions, resulting in a three dimensional polymeric chain, including (i) dissolution of silicon and aluminum atoms through the hydroxide ions reaction, (ii) transportation, orientation and condensation of ions into monomers and (iii) polycondensation/polymerization of monomers into polymeric chains [10]. Basically, the life cycle assessment (LCA) method is used to calculate the range of CO₂ emission of materials, considering all processes such as raw material (natural sources), transportation, manufacturing and use. According to the studies by McLellan et al. [11] and Habert et al. [12], due to the mining, processing, and transport of raw materials, the range of CO₂ emission for GPC is 26%–45% lower compared to cement-based concrete. Numerous researchers have studied the durability of sodium-based (Na-based) GPC [13,14]. However, there are limited studies conducted on the development of mix design, durability and elastic modulus determination of potassium-based (K-based) GPC made using a combination of bottom-ash and fly-ash [15].

The mechanical properties of GPC are influenced by various factors including raw materials, the activator type and molarity [16,17]. Ryu et al. [18] and Khater et al. [19] reported that curing condition also plays a vital role in dissolution and geopolymerization of the aluminum-silicate gel which results in high early strength gain. Therefore, the need for sufficient curing of concrete cannot be overemphasized. According to reported literature [20,21], GPC requires heat treatment in order to attain similar or higher compressive strength in comparison with Portland Cement Concrete (PCC). Yang et al. [22] compared the emission of CO₂ from both GPC and Ordinary Portland Concrete (OPC). The results showed that the total CO₂ emission from heat curing (steam curing at 85 °C for a duration of 24 h) is evaluated at about 38.5 kg/FU, which is quite energy intensive. However, this energy consumption in GPC is reduced in the transportation phase, where the total CO₂ emissions of GPC can be 45% less when compared to its counterpart OPC. In this study two methods of curing (steam and dry) were used to investigate their influence on compressive strength for GPC made using 50% fly-ash and 50% bottom-ash. This presented mix proportion/ratio used in this study was chosen after considering several other proportions in separate studies [23–25] previously completed by the authors and their associates. Sajedi et al. [26] compared the compressive strength of 24 mixes cured with various curing methods including room temperature, in water without heating, room temperature after heating 60 °C for duration of 20 h and in water after heating 60 °C for duration of 20 h. According to the results, due to relatively high consistency of slag when exposed to unheated water, the slag-based mortars showed higher compressive strength (80 MPa) at 90 days compared to other mixes. Parghi et al. [27] investigated the effect of various curing temperatures and curing duration (ambient, moisture curing and submergence curing) on engineering properties of polymer-modified mortars. In accordance to the results, polymer-based mortars (polymer/cement ratio up to 15%) cured for seven days in water submergence and for 21 days in ambient temperature gained higher durability compared to other types of mix composition and curing regime. Parghi et al. [27] attributed this phenomenon to a greater bond strength of both cement particles and polymer films. Heah et al. [28] microstructurally studied the influence of a curing regime on kaolin-based GPC. The samples were cured at temperatures of ambient, 40 °C, 60 °C, 80 °C and 100 °C for one day, and up to three days. The SEM results showed that higher geopolymeric gel and denser matrices was developed for kaolin-based GPC cured at 60 °C up to three days. Moreover, to achieve optimum compressive strength at ambient temperature, it is reported that calcium-based materials such as calcium oxide (CaO) contributes to form hydrated gel including calcium-silicate-hydrates (C-S-H) along with the alumino-silicate gel, where CaO content leads to durable GPC [29]. However, in this study attempts have been made to produce GPC using bottom-ash and fly-ash using heat treatment.

Moreover, establishing a relationship between various mechanical properties of GPC is important for future applications of GPC. The modulus of elasticity is a vital mechanical property of concrete including GPC when compression stress is applied. Modulus of elasticity in concrete refers to the deformation resistance a concrete structure has to loading. That is, elastic modulus evaluates the

stiffness of the concrete. This property is used for design of various structural applications such as high-rise buildings and bridge piers where the stiffness of the concrete is of great importance. Noushini et al. [30] produced class F fly-ash based GPC samples to measure the effect of heat curing on their mechanical properties including compressive strength and elastic modulus. The GPC samples were cured at temperatures of ambient, 60 °C, 75 °C and 90 °C for durations of 8, 12, 18 and 24 h. According to the results, the compressive strength of 62.3 ± 0.2 MPa and elastic modulus of 25.9 GPa was achieved with the increase in the curing temperature up to 75 °C and curing duration up to 24 h. Yang et al. [25] made a correlation between compressive strength and elastic modulus of various mixes. Yang et al. [25] observed that with similar compressive strength (about 30 MPa), heat-cured GPC made using only fly-ash had lower resonant frequency than OPC, which meant a lower modulus of elasticity. However, there are limited studies on the modulus of elasticity of GPC made using bottom-ash [15]. The authors also could not find any work that predicts and compares these values with PCC.

Research Contribution

This study aimed at developing a new type of concrete made using a combination of waste materials including fly-ash and bottom-ash. Even though extensive research has been performed on Na-based GPC made using different precursors [31–35], limited studies are reported in the literature on K-based GPC especially when made using a combination of 50% fly-ash and 50% bottom-ash.

GPC as a material is known to be sensitive to moisture and temperature [17,36]. Moreover, heat treatment has a significant impact on the microstructure and strength development of GPC. Hence, the geopolymerization process is normally dependent on methods of curing. This study is also targeted at experimentally investigating the influence of the heat curing regime on the compressive strength of GPC. Two methods of curing (steam and dry) were used in order to gain similar or higher compressive strength in comparison with PCC. Moreover, it is reported [37,38] that higher curing temperature and curing time result in higher ultimate strength of GPC. In this study, attempts have been made to determine optimum curing temperature and duration for K-based GPC made using fly-ash and bottom-ash.

The elastic modulus is also one of the key mechanical properties of GPC that indicates its ability to deform elastically. A concrete structure needs to have higher compressive strength with a higher elastic modulus to allow carrying of high load values. Otherwise, lower elastic modulus limits the practical applications since the deformations experienced are very high, causing failure of serviceability limits. Since the authors have not found any other work reported in the literature on correlating elastic modulus and compressive strength of K-based GPC made using bottom-ash and fly-ash, in this study attempts have been made to experimentally find a better predictive model for GPC using the proposed empirical formula by other researchers.

2. Experimental Program

2.1. Fly-Ash and Bottom-Ash

Class F fly-ash and bottom-ash used in this study were obtained from pulverized coal combustion from Lafarge Canada Inc. The chemical compositions of bottom-ash and fly-ash (shown in Table 1) were determined by X-ray Diffraction (XRD) technique. The major components in fly-ash and bottom-ash were silicon oxide, aluminum oxide and iron oxide.

Table 1. Chemical composition of fly-ash and bottom-ash. Source: Lafarge Canada Inc.

Chemical Compounds	Fly-Ash (%)	Bottom-Ash (%)
SiO ₂	47.1	60.11
Al ₂ O ₃	17.4	14.35
Fe ₂ O ₃	5.7	5.92
CaO	14	10.40
MgO	5.4	4.49
SO ₃	0.8	0.10
LOI	0.19	0.00
Na ₂ O	N/A	2.232
K ₂ O	N/A	1.766
TiO ₂	N/A	0.892
P ₂ O ₅	N/A	0.200
Mn ₂ O ₃	N/A	0.093

Table 2 shows the physical properties of fly-ash particles measured at the Lafarge Concrete lab. The measured properties are compared with the requirement of ASTM C618 [39]. The physical properties of bottom-ash particles are not evaluated by Lafarge because bottom-ash is not characteristically used in the construction industry. In general, bottom-ash particles are much coarser than fly-ash particles. This is why bottom-ash particles were sieved (#1.18) to eliminate large particles and to increase the surface area of particles to attain optimum strength.

Table 2. Fly-ash physical properties.

	Fly-Ash	ASTM C618 [39]
Fineness retained on 45 µm (No. 325 sieve)	17.3%	<34% (complies)
Strength activity index with Portland cement% of control at 28 days	99%	>75% (complies)
Water requirement, percent of control	100%	<105% (complies)
Autoclave expansion	0.04%	<0.8% (complies)
Density	2.65 Mg/m ³	<5% (complies)

Table 3. shows other properties of fly-ash and bottom-ash obtained from the Material Safety Data Sheets (MSDS) of Lafarge Canada Inc.

Table 3. Other properties of both fly-ash and bottom-ash.

Material	Appearance	Odor	pH	Boiling Point	Specific Gravity	Solubility
Fly-ash	Gray/Black or Brown/Tan (Powder)	odorless	4–12	>1000 °C	2.0–2.9 (water = 1)	Water: <5% (slightly)
Bottom-ash	Gray/Black or Brown/Tan (Powder)	odorless	4–12	>1000 °C	2.0–2.9 (water = 1)	Water: <5% (slightly)

Figure 1 presents the images of both fly-ash and bottom-ash taken by a Hitachi S-4800 Scanning Electron Microscopic (SEM) at the University of Victoria. When using the SEM, accelerating voltage and magnification of 15 KV and 2200x, respectively, were used. Noticeably, diverse shape of bottom-ash particles shown in Figure 1i is visible, ranging from almost impeccably spherical to extremely irregular (rough formed) shaped particles. It can be seen in Figure 1ii that fly-ash particles are glassy and spherical in shape. Moreover, the particle size investigation of bottom-ash and fly-ash performed by the authors showed that the mean size of rounded shaped bottom-ash and fly-ash is 58.53 µm and 10 µm, respectively [40]. The average height and width of the rough formed bottom-ash is 22.59 µm and 12.78 µm, respectively.

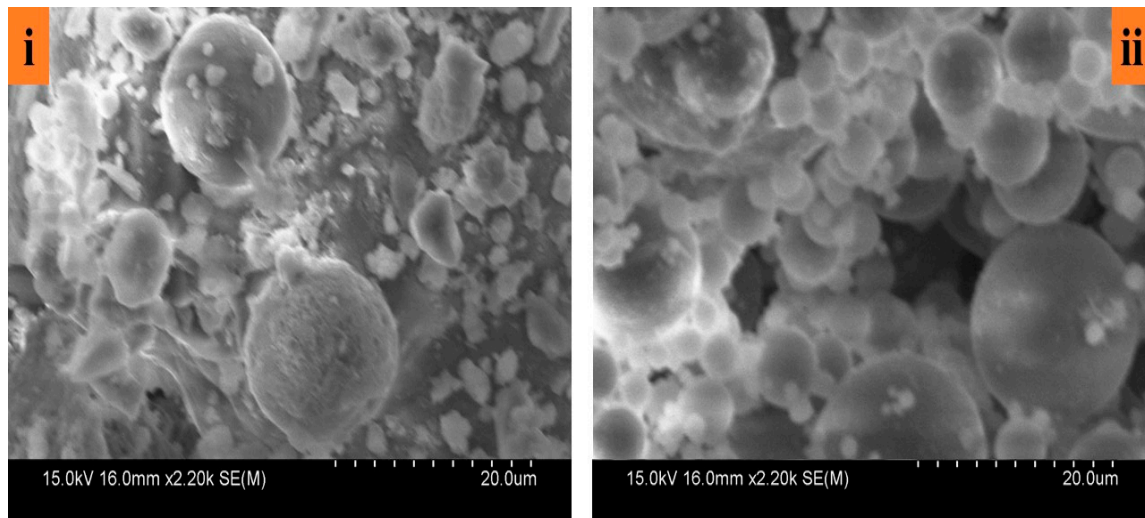


Figure 1. SEM images of (i) bottom-ash (ii) fly-ash.

2.2. Alkaline Liquid and Aggregates

A combination of Potassium Silicate (K_2SiO_3) solution and Potassium Hydroxide (KOH) solution was chosen as the alkaline liquid. KOH solution was prepared using industrial grade KOH flakes obtained from Sigma-Aldrich Private Ltd., Canada. The KOH solution was prepared by dissolving the flakes in water. The mass of KOH solids in a solution varied depending on the concentration of the solution expressed in terms of molarity (M). K_2SiO_3 powder (AgSil 16) obtained from PQ Corporation (USA) was used. Based on the MSDS of the product, the chemical compositions of K_2SiO_3 powder were $K_2O = 32.4\%$, $SiO_2 = 52.8\%$ and water = 14.8% by mass.

GPC was produced with sand and coarse aggregates (with a maximum size of aggregates 12.5 mm) from a quarry in British Columbia, Canada with a relative dry density of 2.67 and 2.71, respectively. The water absorption ratio of sand and coarse aggregates was 0.79% and 0.69%, respectively, in accordance with ASTM C127 [41]. The particle size distribution of coarse and fine aggregates was measured (shown in Figure 2) in accordance with ASTM C33 [42]. Fineness moduli of the coarse and fine aggregates were measured as 6.85 and 3.54, respectively.

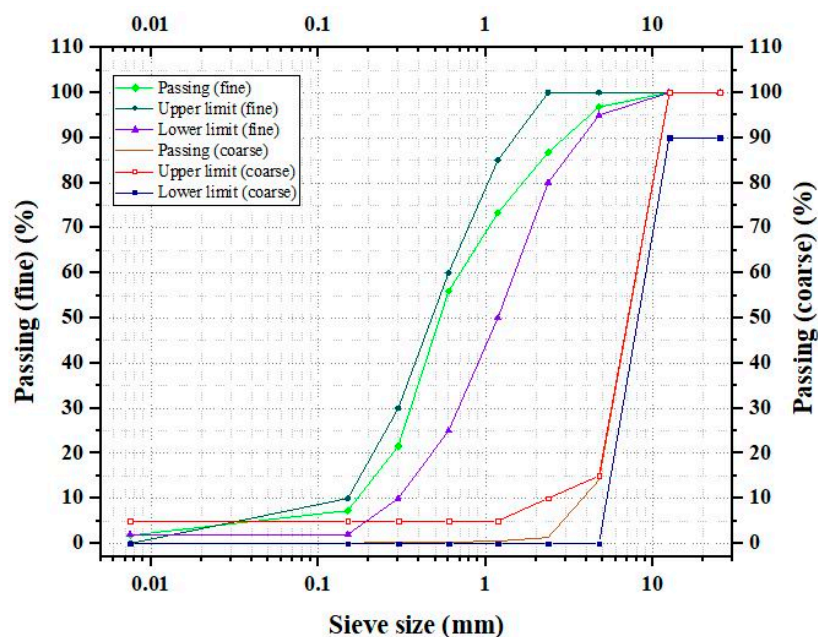


Figure 2. Aggregates' size distribution.

2.3. Mix Proportion

The goal of this study was to compare the performance of the developed GPC with a comparable PCC mix. Since the binders in both PCC and GPC are completely different, their contents had to be varied to achieve a comparable target strength of 35 MPa. The mix proportion of GPC was derived after initial trial experiments on mortars performed in the Facilities for Innovative Materials and Infrastructure Monitoring (FIMIM) by the authors and their associates [23–25].

Table 4 shows the mix proportions of GPC and PCC used in this study. As shown in Table 4, the mass ratio of fly-ash to bottom-ash is 50:50 and the concentration of 12 M was derived after initial testing on GPC. The ratio of alkaline liquid to fly-ash and bottom-ash was selected as 0.21 approximately.

Table 4. Mix Design.

	GPC	PCC
Material	Content (kg/m ³)	Content (kg/m ³)
Fly-ash	194	–
Bottom-ash	194	–
Coarse aggregates	1170	1120
Sand	630	820
KOH (12 M)	85.16	–
K ₂ SiO ₃	125.74	–
Cement (PC)	–	340
Water	38.71	181

Ordinary Portland cement-Type I in accordance with ASTM C150 [43] (referred to as type General Use (GU) in CSA A23.1-14 [44]) was used in the production of PCC. As can be seen in Table 4, the water/cement ratio of approximately 0.53 was selected with a target strength of approximately 35 MPa. The target strength of 35 MPa for both types of concrete was selected as this strength is typically prescribed for several common applications in practice.

3. Method of Casting, Curing and Testing

3.1. Specimen Preparation

Typically, the concrete paste design is critical and depends on the application where it is going to be used. In this study, curing temperature, duration and consequently its effect on the compressive strength of GPC were chosen as the key focus.

In this study, GPC and PCC cylindrical samples were cast and cured as detailed in ASTM C192 [45]. For the manufacturing of GPC, first of all, a combination of K₂SiO₃ and KOH (alkaline solution) was prepared 24 h before mixing. Later, sand and coarse aggregates were placed into a mixer, and the mixing procedure was initiated. After 30 s, both ashes were added to the mix after stopping the mixer. Then, the alkaline solution was added without pausing the mixer. After 30 more seconds, part of extra water (if needed) was added (and noted) to the mixer to achieve the desired workability. After all ingredients were in the mixer, the materials were mixed for 3 min followed by a 3-min rest period, followed by another 2 min of final mixing. After 2–3 min of rest, cylindrical samples (Φ100 × 200 mm) were prepared to measure the compressive strength of mixes cured at various temperatures in both dry and steam curing conditions. After 30 s of vibration of samples on a table vibrator, each cylinder was covered with a plastic sheet to prevent excessive evaporation and kept overnight in the laboratory at ambient temperature.

For PCC, the sequence of mixing was as follows: coarse aggregates and sand were mixed in dry form for 1 min. Then, cement was added to the mixer and mixed for 2 min. After proper mixing of dry

materials, water was gradually added while the mixer was in motion. After adding water, concrete was mixed for 2 min in the mixer, then rested for 1 min, followed by mixing again for 2 min.

3.2. Curing of Samples

Accelerated curing is any method by which high early age strength is achieved in GPC. In this paper, dry and steam curing methods were used to achieve higher compressive strength. Hence, for the dry curing method, GPC specimens were kept in an oven at temperatures of 30 °C, 45 °C, 60 °C, and 80 °C for a period of 24 h and kept at ambient temperature for 28 days. For the steam curing method, samples were kept in a bucket surrounded by water. The bucket was wrapped up tightly to prevent excessive evaporation during the curing process and the bucket was then kept into an oven at temperatures of 30 °C, 45 °C, 60 °C, and 80 °C. Lastly, samples were removed from the oven after 24 h, unwrapped and kept at ambient temperature for 28 days. It is well established that a higher temperature for a longer period of time (up to 72 h) can result in higher strength gain in GPC [37,38]. However, the aim of this study was to expose the specimens to heat curing only for 1 day to reduce the amount of energy utilized for curing. Another goal was to determine the feasibility of using curing temperatures lower than those reported in the literature [46].

The PCC samples were cured by demolding and storing in a water tank at 23 ± 2 °C for 28 days.

3.3. Test Methods

3.3.1. Compressive Strength

A total of 54 GPC and 6 PCC cylindrical samples ($\Phi 100 \times 200$ mm) were tested at an age of 28 days using a Forney compression test machine in accordance with ASTM C39 [47]. The loading rate was between 0.15–0.3 MPa/s.

3.3.2. Dynamic Modulus of Elasticity

To evaluate the dynamic modulus of elasticity of GPC and PCC specimens, an additional 24 samples were cast and cured for 7 and 28 days. The Resonant Frequency Test (RFT) was conducted in accordance with ASTM C215 [48]. The ASTM C215 [48] is often considered for elastic modulus calculation of conventional concrete. However, it should be noted that the elastic modulus of the final element is directly linked to mechanical strength/compressive strength development of the material. Moreover, GPC has almost similar composition as conventional concrete except for the binder. Elastic modulus is known to be highly dependent on the aggregate type and quality. So, procedures in ASTM C215 [48] should also be applicable for determination of the elastic modulus of GPC. Longitudinal impact resonant frequency test was performed on cylindrical specimens of 100 mm diameter and 200 mm height as seen in Figure 3.

The RFT device includes a PCB Integrated Circuit Piezoelectric (ICP) accelerometer (with a pickup sensitivity of 102.2 mV/g (10.2 mV/ms^{-2}) and frequency range of 0.3–15 kHz) that is attached to the concrete sample surface using adhesive wax and a 4 channel NI USB6009 DAQ Analog Digital Converter (ADC) is used for collecting the input compression wave voltage. A standard ball tip hammer weighing 110 ± 2 g with a tip diameter of 10 mm is used to strike the sample surface. A total of 72 readings on 24 samples were taken and outlier were omitted in the average values. National Instrument's LabVIEW 2014 (NI LabVIEW) was used to acquire and analyze the data. The program was developed for this study considering ASTM C215 [48] for acquisition requirements. Table 5 indicates the properties of the accelerometer used in this study.

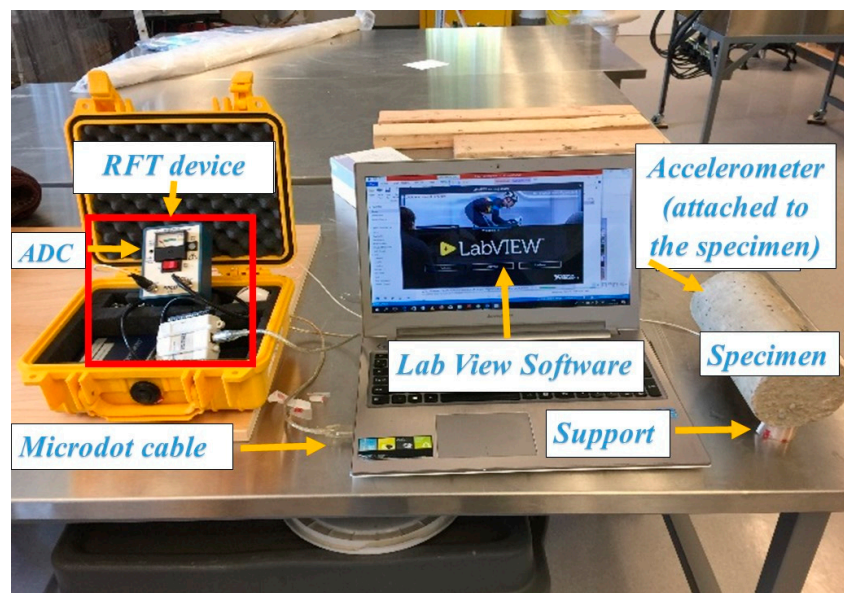


Figure 3. Fundamental longitudinal resonant frequency test.

Table 5. Accelerometer specification.

Type	PCB-ICP
Model	352C33
Height	15.7 mm
Weight	5.8 g
Sensitivity	10.2 mV (m/s ²)
Frequency Range	0.3–15,000 Hz
Non-Linearity	<1%
Transverse Sensitivity	<5%
Temperature Range	−54 to 93 °C

The dynamic elastic modulus was calculated using Equation (1) in accordance with ASTM C215 [48]:

$$E = 5.093 (L/d^2) Mn^2 \quad (1)$$

where:

- E = dynamic elastic modulus (Pa)
- L = length of concrete cylinder (m)
- d = diameter of concrete cylinder (m)
- M = mass of concrete cylinder (kg)
- n = fundamental longitudinal frequency (Hz)

3.3.3. Modulus of Elasticity Predictive Models

Various modulus of elasticity predictive models (discussed below) of different GPC mixtures were compared with the modulus of elasticity of K-based GPC obtained from the experimental results in this study. This was with a goal to identify the most suited model for the material developed in this study.

Hardjito et al. [49] established Equation (2) for calculation of elastic modulus of heat-cured fly-ash based GPC.

$$E_c = 2707 \sqrt{f_{cm}} + 5300 \quad (2)$$

E = Modulus of elasticity (MPa)

$f_c = f' = f_m$ = Compressive strength (MPa)

ρ = Density (kg/m^3)

The aforementioned variables and units are used henceforth.

Hardjito and Rangan [50] made a comparison between experimental values of elastic modulus of fly-ash based GPC, the empirical formula proposed by AS 3600 [51] and ACI Committee 363 [52]. The elastic modulus of specimens was measured in accordance with the Australian Standard AS 1012.17 [53]. According to the results, experimental values were lower than the proposed model due to the granite-type coarse aggregates used in the experimental results. The formula proposed by AS 3600 [51] was not used in the current study because it is established for concrete that has compressive strength greater than 40 MPa. Hardjito and Rangan [53] recommended that the ACI 363 [52] model (Equation (3)) is better for calculating the modulus of elasticity.

$$E_c = 3320 \sqrt{f'_c} + 6900 \quad (3)$$

Tempest et al. [54] proposed Equation (4) to calculate the elastic modulus of fly-ash based GPC. The modulus of elasticity of samples was evaluated using the procedure given in ASTM C469 [55]. The results showed that the elastic modulus increases as the compressive strength of GPC increases. It was also found that experimental values have the same trend (slightly higher) as the proposed formula.

$$E_c = 3421 \sqrt{f'_c} \quad (4)$$

Prachasaree et al. [56] measured the static modulus of elasticity of specimens in accordance with ASTM C469 [55]. They used a predictive model proposed by Hardjito et al. [49], ACI 318 [57] and ACI 363 [52] to calculate the elastic modulus of GPC. However, it is stated that all the proposed formulas do not fit the experimental results. Therefore, they proposed Equation (5) for calculation of elastic modulus of fly-ash based GPC.

$$E = 840 - 886 \sqrt{f_c} + 647 f_c \quad (5)$$

Thomas and Peethamparan [58] proposed two equations for the prediction of elastic modulus from compressive strength using ASTM C469 [55]. The difference between these two equations was not clearly stated in their study. The proposed equation by ACI 318 [57] was compared with Equations (6) and (7). The results showed that both Equations (6) and (7) vary slightly from ACI 318 [57] in terms of predicted values and goodness of fit. However, authors mentioned that due to variation in the data, additional investigation is needed to find a better fitting formula.

$$E = 2900 f_c^{3/5} \quad (6)$$

$$E = 4400 \sqrt{f_c} \quad (7)$$

Wardhono [59] compared the experimental results of modulus of elasticity of fly-ash based GPC with proposed equations by Ng and Foster [60], AS 3600 [51] and Diaz-Loya et al. [61]. It is reported that AS 3600's model with higher R^2 (98.13%) showed a closest and similar trend to experimental values. However, only five specimens were used to determine the modulus of elasticity of fly-ash based GPC at different ages including 28, 90, 180, 360, 540 days. In this study, Equation (8) was established for the determination of elastic modulus.

$$E_c = f_c^{1.6412} 49.968 \quad (8)$$

Gunasekara et al. [62] made a correlation between elastic modulus and compressive strength of fly-ash based GPC using equations proposed by Hardjito and Rangan [50], Diaz-Loya [61], Olivia and Nikraz [63] and Wardhono [59]. They also compared the determined formula with AS 3600 [51]. The static modulus of elasticity of samples was measured in accordance with AS 1012.17 [53]. It is

reported that AS 3600 [51] overestimated the experimental results of GPC. Equation (9) was developed for the determination of elastic modulus:

$$E_c = \rho^{1.5} 0.024 \sqrt{f_c} \quad (9)$$

In this study, all the predictive models reported above have been compared to test results presented later in this manuscript.

4. Results and Discussion

4.1. Workability and Density

The slump test was performed immediately after preparing the mixes to measure the workability of fresh paste in accordance with ASTM C143 [64]. In this study, the slump value of K-based GPC and PCC was 185 mm and 210 mm, respectively. It is reported that GPC and PCC are considered to be highly workable when GPC and PCC gain a slump value over 90 mm and 180 mm, respectively [65,66]. These two types of concrete with high workability are very easy to mix, transport, place and compact in structures. K-based GPC showed lower workability compared to its counterpart PCC because of the existence of silicates in GPC which increases the viscosity characteristic of the paste and makes GPC more cohesive and stickier than PCC [67,68].

The average dry density of three PCC and GPC samples at seven days and 28 days was measured. The results showed that the average density of GPC increased from 2430 kg/m³ at seven days to 2437 kg/m³ at 28 days with an overall increase of 0.28%, while the average density of PCC increased from 2453 kg/m³ at 7 days to 2462 kg/m³ at 28 days with an overall increase of 0.36%. These results can be attributed to the microstructure of bottom-ash particles, where large size and irregularly-shaped particles of bottom-ash caused GPC to be ever so slightly less dense and nonhomogeneous than PCC [15]. Moreover, this finding is in good agreement with the study of Chindaprasirt et al. [7] and Haq et al. [9] where bottom-ash based GPC showed lower dry density due to the excessive evaporation of residual liquid such as water and alkaline solution over the curing process.

4.2. Effect of Heat Treatment on Compressive Strength of GPC Samples

As mentioned earlier, in this study the compressive strength of hardened concrete was selected as the performance criteria. Generally, longer curing time enhances the polymerization process resulting in higher compressive strength. In this study, five different curing temperatures were used, i.e., ambient, 30 °C, 45 °C, 60 °C, 80 °C. Figure 4 presents the average compressive strength of steam and dry-cured samples. The results are reported as an average of six samples along with error bars. Figure 4 indicates that the compressive strength of steam-cured samples increased about 3.5 times when the temperature went from ambient temperature (~10 °C) to 80 °C. In comparison, the compressive strength increased approximately 2.3 times when specimens were dry-cured. Figure 4 also shows that the temperature of 80 °C during the steam curing method resulted in higher compressive strength. Based on the results of compressive strength, steam curing at the temperature of 80 °C was chosen in this study as the preferred method of curing.

According to other studies on the microstructure of GPC [69,70], the steam curing method improves the dissolution rate of chemical species, such as Silicon Dioxide (SiO₂) and Aluminum Oxide (Al₂O₃), from paste where the rate of geopolymerization increases. This finding can be attributed to the full and uniform internal curing of specimens. Abdollahnejad et al. [71] microstructurally investigated the effect of thermal curing on fly-ash based GPC. The results showed that thermal treatment causes denser paste and less cracks due to the higher degree of reaction and higher adhesion between the amorphous gel and the particles. It should be noted that an increase in compressive strength is typically not expected to be achieved beyond a temperature of 80 °C [72], hence this was established as the upper bound for curing temperature in this study.

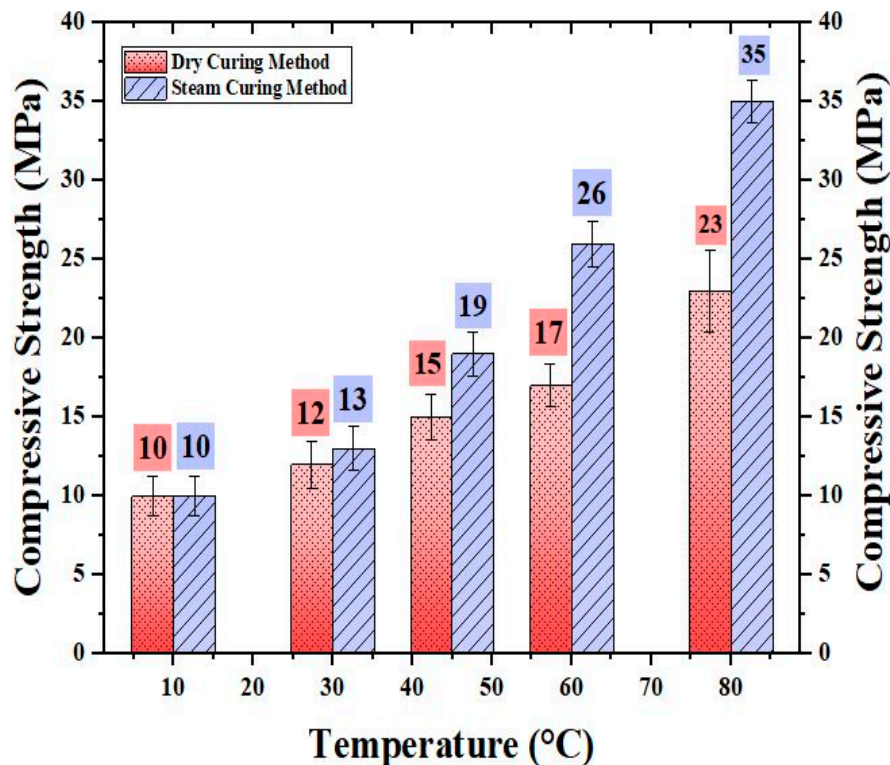


Figure 4. Average compressive strength of steam-cured geopolymer concrete (GPC) samples.

Figure 4 also reveals that at the same curing temperature, steam-cured samples yielded a higher strength than that of dry-cured samples. This can be attributed to the existence of the adequate amount of water during the geopolymerization process, while, in the dry curing method, an excessive amount of water evaporated quickly from samples and there was not enough water in the samples for complete geopolymer formation [73]. Generally, the geopolymerization process is accelerated at the higher temperature [74]. In this study, ambient-cured GPC samples did not develop adequate compressive strength at an age of 28 days because GPC paste reacts slowly and takes considerably long time to set at ambient/low temperature compared to heat-cured samples [75]. However, it is suggested to add calcium-based materials (such as cement and slag) in GPC mixture to improve engineering properties of ambient-cured GPC since it is more practical in-situ to cure samples at ambient temperature [29,76].

Provis et al. [77] reported that the Na-based solution is mostly used because of its availability, low cost, and high reactivity. However, the K-based solution is considered for high temperature applications [78,79]. Hounsi et al. [80] reported that Na-based GPC has lower compressive strength value than K-based GPC at the same alkaline concentration of the current study (12 M) due to the reduction of Si/Na ratio at high concentration of sodium hydroxide (NaOH), where NaOH slows the polycondensation process and damages the mechanical properties of Na-based GPC.

Average compressive strength of 31 MPa and 33 MPa for PCC was measured at an age of 7 days and 28 days, respectively. This was most comparable to the strength of steam-cured GPC samples at 80 °C.

It is reported that the compressive strength of 17 MPa is appropriate for residential buildings and compressive strength of 28 MPa and higher is proper for commercial buildings [81]. Greater compressive strength up to and beyond 70 MPa is stated for other applications such as dams [81]. Therefore, selected compressive strength/temperature (35 MPa/80 °C) in this study provides and meets a wide range of requirements for applications including residential and commercial. However, it should be mentioned that GPC samples can be either dry-cured or steam-cured at 60 °C for some applications and it may not be necessary to cure at a high temperature such as 80 °C.

It is well-known that only ambient temperature curing is a practical method in the construction of concrete buildings or other structures. Hence, according to Nath et al. [82], using calcium-based material such as cement enhances setting time, workability and durability of GPC cured at ambient temperature. The microstructural investigation of high-calcium-based GPC indicated that both sodium aluminosilicate hydrate (N-A-S-H) and calcium aluminosilicate hydrate (C-A-S-H) gel are formed in high-calcium-based GPC [71]. This phenomenon is reported by other studies [71,83,84], where silica content, calcium content and aging conditions affect the phase transition behavior of fly-ash based GPC. Abdollahnejad et al. [71] reported that the samples with higher molar ratio of Na/Ca achieved higher rates compared to other samples with molar ratio of Si/Al and Ca/Si in terms of gel formation at the ambient temperature (25 °C and 30% relative humidity). Thus, the replacement of calcium by sodium causes ionic exchange mechanisms, where sodium species are replaced by calcium ions (Ca^{2+}) in C-A-S-H gel, and (C,N)-A-S-H gel is formed [71]. This replacement causes a denser paste and decreases crack creation. Abdollahnejad et al. [84] replaced 10%, 20%, and 30% ceramic wastes with slag to produce GPC, containing coarse porcelain ceramic waste as aggregate. Two methods of the curing regime include sealing with plastic and thermal curing conditions for 3 h at 60 °C to cure the samples. According to the results, lower amounts of calcium content caused a reduction in compressive strength of GPC samples.

4.3. Longitudinal Resonant Frequency

The average resonant frequency of six GPC and six PCC specimens was calculated. Figure 5 shows the values of resonant frequency versus compressive strength at an age of seven and 28 days, respectively. It can be seen in Figure 5 that the resonant frequency of both types of concrete increased gradually as the age increased due to the continuous geopolymerization/hydration process. According to the results, after 28 days of curing, GPC showed a moderate increase (~2.47%) in average resonant frequency values when compared to seven day values as specimens aged with developing microstructure between seven and 28 days. Compared to this, PCC showed a smaller increase (~0.74%) possibly due to almost fully completed hydration within seven days.

Typically, the resonant frequency increases as the compressive strength increases. That is why, due to the higher compressive strength, PCC samples showed higher resonant frequency (as shown in Figure 5) compared to its counterpart GPC at both seven and 28 days.

It also can be seen in Figure 5 that the resonant frequency of GPC ranges from 7000 to 8000 Hz, whereas for PCC it ranges from 8000 to 9100 Hz. The calculated standard deviation of GPC and PCC was 220.65 and 144.86, respectively, at seven days, whereas the calculated standard deviation of GPC and PCC was 178.69 and 161.18, respectively, at 28 days. This phenomenon is in good-agreement with previous studies performed at the University of Victoria [25,85] by the authors, where with average compressive strength of 20–30 MPa and the average longitudinal resonant frequency of PCC and GPC was about 9000–9500 Hz and 5500–6000 Hz, respectively. According to a study by Massoud et al. [86], GPC specimens have a lower frequency than PCC for mixes that have a similar average 28 days compressive strength due to elevated curing condition and internal moisture loss.

Equation (1) was used to calculate the elastic modulus of GPC and PCC samples at an age of seven days and 28 days. Then, a correlation between compressive strength and modulus of elasticity was derived (Figure 6). It can be seen in Figure 6 that a slight overall increase in compressive strength of PCC resulted in a much larger increase in the overall value of dynamic modulus of elasticity approximately ranging from 27 GPa to 33 GPa. However, GPC showed a minor increase of the dynamic modulus of elasticity, approximately ranging from 20 GPa to 24 GPa, with an increasing of compressive strength from 30 MPa to 35 MPa. The standard deviation value of GPC and PCC was 1.24 and 0.76, respectively, at seven days, while the standard deviation value of GPC and PCC was 0.85 and 0.96, respectively, at 28 days. This is a very interesting finding and is in good agreement with Fernandez-Jimenez et al.'s study [87] where with a similar compressive strength the elastic modulus of fly-ash based GPC was in the range of 10–20 GPa, while cement-based concrete had a higher elastic modulus in the

range of 25–35 GPa. According to Duxson et al. [88] and Sofi et al. [89], the elastic modulus of GPC depended on the $\text{SiO}_2/\text{Al}_2\text{O}_3$ ratio, mix proportion and curing method. However, both Sofi et al. [89] and Duxson et al. [88] reported that the elastic modulus of GPC varied from 10–55 GPa, which covers the values of elastic modulus of GPC reported in this research. The aforementioned issue indicates that Equation (1) is applicable for cement-based concrete, and this equation overestimated the dynamic elastic modulus of GPC owing to the higher resonant of PCC [25].

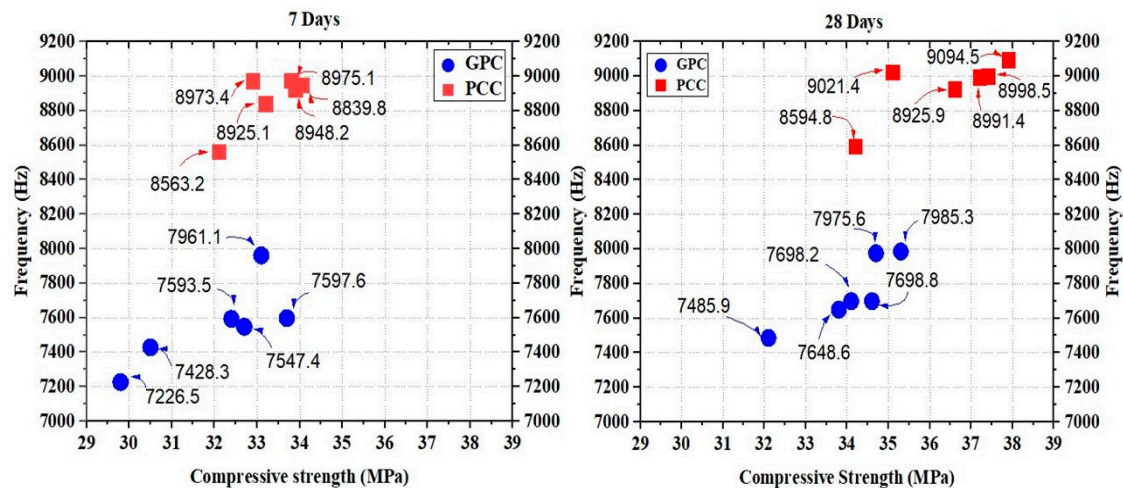


Figure 5. Compressive strength of GPC and Portland Cement Concrete (PCC) vs. Frequency.

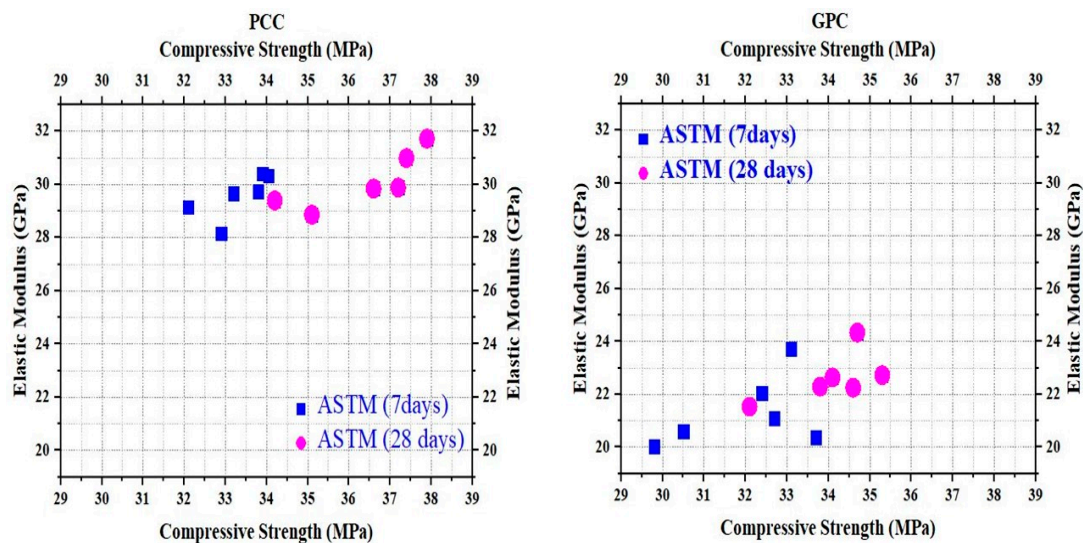


Figure 6. Elastic modulus versus compressive strength.

It should be noted that the use of a higher amount of coarse aggregates in the mix proportion may increase/decrease the elastic modulus of concrete. In this study, due to the use of different types of concrete (GPC and PCC) and variation of the mix proportions, slightly higher content of coarse aggregates (4.36%) was used in GPC compared to PCC to achieve a compressive strength of 35 MPa. However, as is the case in this study, the elastic modulus of GPC is generally reported less than its counterpart PCC [87,89]. This phenomenon can be attributed to various factors including microstructure of concretes (porosity), strength, paste, elastic modulus of raw materials, characteristics of the transition zone, aggregates, etc. [20].

According to the Nath et al. study [90], the elastic modulus of ambient-cured GPC is about 25%–30% less compared to cement-based concrete at 28 days. It can be noted that both types of curing

methods (heat curing and ambient curing) create GPC of lower elastic modulus compared to that of cement-based concrete.

In this study, material-focused investigation of both types of concrete showed that mixtures' stiffness/compressive strength increases with time (Figure 6). This is attributed to the increasing strength over curing time. However, in a concrete building after a brief period of time, this tendency becomes negligible due to the sustained loads (self-weight, dead loads and live loads) [91]. This is why it is significant to investigate the elastic modulus of materials when real loads are applied because the elastic modulus of concrete is relatively constant at low stress levels but starts decreasing at higher stress levels.

4.4. Comparison between Predicted and Experimental Modulus of Elasticity

In this study, the experimental results were compared with the predictive models (Table 6) proposed by other researchers to identify the best suited model for this type of mixture containing bottom-ash.

Table 6. Equations and establishers.

Equation	Establisher
$E_c = 2707 \sqrt{f_{cm}} + 5300$	Hardjito et al.
$E_c = 3320 \sqrt{f_{cm}} + 6900$	ACI 363 (Hardjito and Rangan)
$E_c = 3421 \sqrt{f'_c}$	Tempest et al.
$E = 840 - 886 \sqrt{f_c} + 647f_c$	Prachasaree et al.
$E = 2900f_c^{3/5}$	Thomas and Peethamparan
$E = 4400 \sqrt{f_c}$	Thomas and Peethamparan
$E_c = f_c^{1.6412} 49,968$	Wardhonoet al.
$E_c = \rho^{1.5} 0.024 \sqrt{f_c}$	Gunasekara et al.

The experimental results for average modulus of elasticity (from experimental results) of six GPC specimens at an age of seven and 28 days are indicated in Figure 7. It should be noted that all of the proposed models considered in this study are for GPC made only with fly-ash. However, bottom-ash has similar physical, chemical and mechanical properties as fly-ash [92]. One would expect that these models are also applicable for GPC made using a combination of bottom-ash and fly-ash as well. Figure 7 shows the elastic modulus of GPC achieved from experimental results and predictive models.

The aforementioned Equations (2)–(9) were proposed to calculate the static elastic modulus from the compressive strength of GPC. It should be mentioned that the authors could not find any predictive models for the dynamic elastic modulus of K-based GPC made using a combination of fly-ash and bottom-ash. However, Yang et al. [25] and Wongpa et al. [93] reported that static predictive models can reasonably predict the dynamic modulus of elasticity because the predicted values are consistently lower or higher than the experimental values. Moreover, Yang et al. [25] used Kar et al.'s work [94] to develop a relationship between compressive strength and dynamic elastic modulus. According to their results, the maximum compressive strength difference between Yang's model [25] and Kar et al.'s model [94] was about 3.49 MPa when dynamic elastic modulus was about 23.69 GPa. Moreover, the values of static predictive models and the dynamic predictive models were in close agreement and had a similar trend.

In this study, an average of three readings were taken for each GPC sample to calculate the elastic modulus. A comparison between predictive models reported in previous studies for fly-ash-based GPC and the current study indicates that all models have a similar trend toward increasing elastic modulus with increased compressive strength. Even though there are some differences in compositions of GPCs, as can be seen in Figure 7, all of the predictive models achieved lower elastic modulus values than the experimental values in this study. The elastic modulus values obtained by Wardhono et al. [59]

and Gunasekara et al. [62] are lower than experimental results of GPC made using fly-ash and bottom-ash. Authors attribute the low values in Gunasekara's model [62] to the effect of specific gravity of bottom-ash and fly-ash on density of GPC, which is lower compared to cement-based concrete. Authors believe that Wardhono's model [59] may not be very accurate due to the small sample size of data.

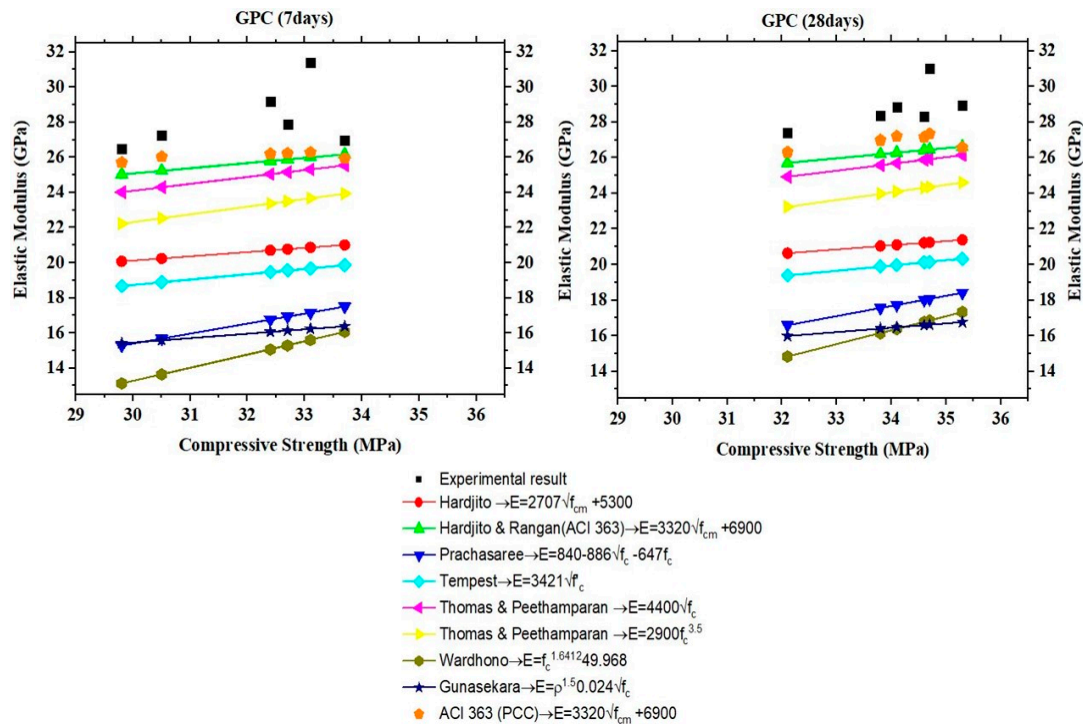


Figure 7. Comparison between predicted and experimental modulus of elasticity.

As can be seen in Figure 7, the ACI 363 [52] model is the closest to the experimental results at both seven and 28 days. In the current study, the average calculated modulus of elasticity of GPC obtained by ACI's model is 8.88% (7 days) and 8.76% (28 days) lower compared to the respective average experimental results at the same age. Hence, the modulus of elasticity for GPC made using fly-ash and bottom-ash can equitably be calculated with reasonable correlation using Equation (3). Moreover, Figure 7 also shows that the model proposed by Thomas and Peethamparan [58] has an average elastic modulus of 11.68% (7 days) and 10.83% (28 days) lower than average experimental results at the same age. Hence, this model could also be used for this type of GPC with reasonable accuracy. It is well-known that ACI 363 [52] is applicable to PCC. However, the predictive model proposed by ACI 363 [52] was also used to make a comparison between the trend of GPC and PCC. It can be seen that the PCC values are slightly higher than GPC values. It shows that ACI 363 [52] marginally overestimated the elastic modulus of GPC. The authors propose the following empirical model to correlate the elastic modulus and compressive strength with a coefficient of determination (R^2) of 0.79.

$$E = 1.76 (f_c)^{0.64} \quad (10)$$

where f_c has the unit of MPa and the unit of "E" is GPa.

5. Conclusions

In this study, the effect of curing temperature on compressive strength and dynamic modulus of elasticity of K-based GPC was investigated. A combination of fly-ash and bottom-ash was used in order to develop a sustainable concrete mix. The comparative results of the study are summarized below:

1. Compressive strength increased approximately 3.5 times when steam-cured temperature increased from ambient to 80 °C. Compressive strength increased approximately 2.3 times when specimens were dry-cured at the same temperature range. Hence, steam curing is preferable to dry curing if rapid strength development is required.
2. The measured values of the resonant frequency of K-based GPC (~7200–9000 Hz) with a compressive strength of 35 MPa was lower than that of cement-based concrete (~8000–9100 Hz) of 35 MPa due to the elevated temperature condition and internal moisture loss.
3. The dynamic modulus of elasticity of bottom-ash based GPC was about 20–24 GPa at an age of 7 days and 28 days. Contrary to this, PCC showed a higher value of elastic modulus that ranged from 27 to 33 GPa.
4. Several predictive models for fly-ash based GPC proposed by other researchers were used to find a model suitable for bottom-ash based GPC. The models proposed by ACI 363 [52] and Thomas et al. [58] were in good agreement with the average elastic modulus of GPC specimens in this study.

Author Contributions: P.A. made different mix propositions and produced all the samples to find the higher compressive strength for this type of concrete. He also performed the compressive strength tests and resonant frequency tests to investigate and estimate the durability of K-based GPC made using fly-ash and bottom-ash. R.G. was the principal investigator on this project who conceptualized this project and was responsible to secure funding for this project. He was responsible to provide the materials, equipment and the test facility including supervision on this project. P.A. wrote the first draft of this paper and R.G. revised it. All authors have read and agreed to the published version of the manuscript.

Funding: This research was funded by India Canada Research Centre of Excellence (IC-IMPACTS).

Acknowledgments: The authors gratefully acknowledge the financial support from IC-IMPACTS for this project and would like to express their special thanks to Matt Dalkie, technical services engineer of Lafarge Canada Inc. and Mike McDonald, field chemist of National Silicates an affiliate of PQ Corporation Company for providing materials for this study.

Conflicts of Interest: The authors declare no conflict of interest.

References

1. Turner, L.K.; Collins, F.G. Carbon dioxide equivalent (CO₂) emission: A comparison between geopolymers and OPC cement concrete. *Constr. Build. Mater.* **2013**, *43*, 125–130. [[CrossRef](#)]
2. Gartner, E. Industrially interesting approaches to “low CO₂” cements. *Cem. Concr. Res.* **2004**, *34*, 1489–1498. [[CrossRef](#)]
3. Wallah, S. Creep behavior of fly-ash based geopolymer concrete. *Civ. Eng. Dimens.* **2010**, *12*, 73–78.
4. Dwivedi, A.; Jain, M.K. Fly ash-waste management and overview: A Review. *Recent Res. Sci. Technol.* **2014**, *6*, 30–35.
5. Environmental Protection Agency. *Regulatory Determination on Wastes from the Combustion of Fossil Fuels*; Environmental Protection Agency: Washington, DC, USA, 2000.
6. American Coal Ash Association. *Coal Combustion Product Production & Use Survey Report*; American Coal Ash Association: Farmington Hills, MI, USA, 2018.
7. Chindaprasirt, P.; Jaturapitakkul, C.; Chalee, W.; Rattanasak, U. Comparative Study on the characteristics of fly-ash and bottom-ash geopolymers. *Waste Manag.* **2009**, *29*, 539–543. [[CrossRef](#)]
8. Sinha, D.K.; Kumar, A.; Kumar, S. Development of Geopolymer Concrete from Fly Ash and Bottom Ash Mixture. *J. Trans. Indian Ceram. Soc.* **2014**, *73*, 143–148. [[CrossRef](#)]
9. Ul Haq, E.; Padmanabhan, S.K.; Licciulli, A. Synthesis and characteristics of fly ash and bottom ash based geopolymers—A comparative study. *Ceram. Int.* **2014**, *40*, 2965–2971. [[CrossRef](#)]
10. Duxson, P.; Fernández-Jiménez, A.; Provis, J.L.; Lukey, G.C.; Palomo, A.; van Deventer, J.S. Geopolymer technology: The current state of the art. *J. Mater. Sci.* **2007**, *42*, 2917–2933. [[CrossRef](#)]
11. McLellan, B.C.; Williams, R.P.; Lay, J.; Van Riessen, A.; Corder, G.D. Costs and carbon emissions for geopolymer pastes in comparison to ordinary Portland cement. *J. Clean. Prod.* **2011**, *19*, 1080–1090. [[CrossRef](#)]

12. Habert, G.; De Lacaillerie, J.D.E.; Roussel, N. An environmental evaluation of geopolymer based concrete production: Reviewing current research trends. *J. Clean. Prod.* **2011**, *19*, 1229–1238. [[CrossRef](#)]
13. Okoye, F.N.; Durgaprasad, J.; Singh, N.B. Fly ash/Kaolin based geopolymer green concretes and their mechanical properties. *Data Brief* **2015**, *5*, 739–744. [[CrossRef](#)] [[PubMed](#)]
14. Shaikh, F.U.A. Mechanical and durability properties of fly ash geopolymer concrete containing recycled coarse aggregates. *Int. J. Sustain. Built Environ.* **2016**, *5*, 277–287. [[CrossRef](#)]
15. Xie, T.; Ozbakkaloglu, T. Behavior of low-calcium fly and bottom ash-based geopolymer concrete cured at ambient temperature. *Ceram. Int.* **2015**, *41*, 5945–5958. [[CrossRef](#)]
16. Zhuang, X.Y.; Chen, L.; Komarneni, S.; Zhou, C.H.; Tong, D.S.; Yang, H.M.; Yu, W.H.; Wang, H. Fly ash-based geopolymer: Clean production, properties and applications. *J. Clean. Prod.* **2016**, *125*, 253–267. [[CrossRef](#)]
17. Part, W.K.; Ramli, M.; Cheah, C.B. An overview on the influence of various factors on the properties of geopolymer concrete derived from industrial by-products. *Constr. Build. Mater.* **2015**, *77*, 370–395. [[CrossRef](#)]
18. Ryu, G.S.; Lee, Y.B.; Koh, K.T.; Chung, Y.S. The mechanical properties of fly ash-based geopolymer concrete with alkaline activators. *Constr. Build. Mater.* **2013**, *47*, 409–418. [[CrossRef](#)]
19. Khater, H. Effect of calcium on geopolymerization of aluminosilicate wastes. *J. Mater. Civ. Eng.* **2011**, *24*, 92–101. [[CrossRef](#)]
20. Mehta, P.K.; Monteiro, P.J. *Concrete Microstructure, Properties and Materials*, 4th ed.; MC-Graw Hill: New York, NY, USA, 2014.
21. Sinan, E.A.; Erdoğan, T. Alkali activation of a slag at ambient and elevated temperatures. *Cem. Concr. Compos.* **2012**, *34*, 131–139.
22. Yang, K.H.; Song, J.K.; Song, K.I. Assessment of CO₂ reduction of alkali-activated concrete. *J. Clean. Prod.* **2013**, *39*, 265–272. [[CrossRef](#)]
23. Gupta, R.; Rathod, H. Current state of K-based geopolymer cements cured at ambient temperature. *Emerg. Mater. Res.* **2015**, *4*, 125–129. [[CrossRef](#)]
24. Belforti, F.; Azarsa, P.; Gupta, R.; Dave, U. Effect of Freeze-thaw on K-based geopolymer concrete and portland cement concrete. In Proceedings of the 6th Nirma University International Conference on Engineering, Ahmedabad, India, 23–25 November 2017.
25. Yang, C.; Gupta, R. Prediction of the compressive strength from resonant frequency for low-calcium fly ash-based geopolymer concrete. *J. Mater. Civ. Eng.* **2018**. [[CrossRef](#)]
26. Fathollah, S. Effect of curing regime and temperature on the compressive strength of cement-slag mortars. *Constr. Build. Mater.* **2012**, *36*, 549–556.
27. Parghi, A.; Shahria Alam, M. Effects of curing regimes on the mechanical properties and durability of polymer-modified mortars—An experimental investigation. *J. Sustain. Cem. Based Mater.* **2016**, *5*, 324–347. [[CrossRef](#)]
28. Heah, C.Y.; Kamarudin, H.; Al Bakri, A.M.; Binhussain, M.; Luqman, M.; Nizar, I.K.; Ruzaidi, C.M.; Liew, Y.M. Effect of Curing Profile on Kaolin-based Geopolymers. *Phys. Procedia* **2011**, *22*, 305–311. [[CrossRef](#)]
29. Yip, C.K.; Lukey, G.C.; Provis, J.L.; van Deventer, J.S. Effect of calcium silicate sources on geopolymerization. *Cem. Concr. Res.* **2008**, *38*, 554–564. [[CrossRef](#)]
30. Noushini, A.; Castel, A. The effect of heat-curing on transport properties of low-calcium fly ash-based geopolymer concrete. *Constr. Build. Mater.* **2016**, *112*, 464–477. [[CrossRef](#)]
31. Arenas, C.; Luna-Galiano, Y.; Leiva, C.; Vilches, L.F.; Arroyo, F.; Villegas, R.; Fernández-Pereira, C. Development of a fly ash-based geopolymeric concrete with construction and demolition wastes as aggregates in acoustic barriers. *Constr. Build. Mater.* **2017**, *134*, 433–442. [[CrossRef](#)]
32. Temuujin, J.; van Riessen, A.; MacKenzie, K.J.D. Preparation and characterization of fly ash based geopolymer mortars. *Constr. Build. Mater.* **2010**, *24*, 1906–1910. [[CrossRef](#)]
33. Chindaprasirt, P.; Chareerat, T.; Sirivivatnanon, V. Workability and strength of coarse high calcium fly ash geopolymer. *Cem. Concr. Compos.* **2007**, *29*, 224–229. [[CrossRef](#)]
34. Lee, N.; Lee, H. Setting and mechanical properties of alkali-activated fly ash/slag concrete manufactured at room temperature. *Constr. Build. Mater.* **2013**, *47*, 1201–1209. [[CrossRef](#)]
35. Görhan, G.; Kürklü, G. The influence of the NaOH solution on the properties of the fly ash-based geopolymer mortar cured at different temperatures. *Compos. Part B Eng.* **2014**, *58*, 371–377. [[CrossRef](#)]
36. Singh, B.; Ishwarya, G.; Gupta, M.; Bhattacharyya, S.K. Geopolymer concrete: A review of some recent developments. *Constr. Build. Mater.* **2015**, *85*, 78–90. [[CrossRef](#)]

37. Memon, F.A.; Nuruddin, M.F.; Demie, S.; Shafiq, N. Effect of Curing Conditions on Strength of Fly ash-based Self-Compacting Geopolymer Concrete. *Int. J. Civ. Environ. Eng.* **2011**, *5*, 342–345.
38. Nurrudin, M.F.; Sani, H.; Mohammed, B.S.; Shaaban, I. Methods of curing geopolymer concrete: A review. *Int. J. Adv. Appl. Sci.* **2018**, *5*, 31–36. [[CrossRef](#)]
39. ASTM C618/C618M. *Standard Specification for Coal Fly Ash and Raw or Calcined Natural Pozzolan for Use in Concrete*; American Society for Testing and Materials: West Conshohocken, PA, USA, 2017.
40. Azarsa, P.; Gupta, R. Novel approach to microscopic characterization of cryo formation in air voids of concrete. *Micron* **2019**, *122*, 21–27. [[CrossRef](#)] [[PubMed](#)]
41. ASTM C127/C127M. *Standard Test Method for Relative Density (Specific Gravity) and Absorption of Coarse Aggregate*; American Society for Testing and Materials: West Conshohocken, PA, USA, 2015.
42. ASTM C33/C33M. *Standard Specification for Concrete Aggregates*; American Society for Testing and Materials: West Conshohocken, PA, USA, 2015.
43. ASTM C150/C150M. *Standard Specification for Portland Cement*; American Society for Testing and Materials: West Conshohocken, PA, USA, 2017.
44. CSA A23.1. *Standard for Concrete Materials and Methods of Concrete Construction*; Canadian Standard Association: Toronto, ON, Canada, 2014.
45. ASTM C192/C192M. *Standard Practice for Making and Curing Concrete Test Specimens in the Laboratory*; American Society for Testing and Materials: West Conshohocken, PA, USA, 2015.
46. Satpute Manesh, B.; Wakchaure Madhukar, R. and Patankar Subhash, V. Effect of Duration and Temperature of Curing on Compressive Strength of Geopolymer Concrete. *Int. J. Eng. Innov. Technol. (IJEIT)* **2012**, *1*, 152–155.
47. ASTM C39/C39M. *Standard Test Method for Compressive Strength of Cylindrical Concrete Specimens*; American Society for Testing and Materials: West Conshohocken, PA, USA, 2014.
48. ASTM C215/C215M. *Standard Test Method for Fundamental Transverse, Longitudinal, and Torsional Resonant Frequencies of concrete specimens*; American Society for Testing and Materials: West Conshohocken, PA, USA, 2014.
49. Hardjito, D.; Wallah, S.E.; Sumajouw, D.M.J.; Rangan, B.V. The stress-strain behaviour of fly-ash based geopolymer concrete. *Dev. Mech. Struct. Mater.* **2005**, *35*, 831–834.
50. Hardjito, D.; Rangan, B.V. *Development and Properties of Low-Calcium Fly Ash-Based Geopolymer Concrete*; Curtin University of Technology: Perth, Australia, 2005.
51. AS 3600. *Concrete Structure*; Standards Australia, Homebus (NSW Australia): Sydney, Australia, 2009.
52. ACI 363. *State of the Art Report on High Strength Concrete*; ACI Committee: Detroit, MI, USA, 1992.
53. AS 1012.17. *Determination of the Static Chord Modulus of Elasticity and Poisson's Ratio of Concrete Specimens*; Australian Standard: Sydney, Australia, 1997.
54. Tempest, B. Engineering characterization of waste derived geopolymer cement concrete for structural applications. *Dissertation Abstr. Int.* **2010**, *71*.
55. ASTM C469/C469M. *Standard Test Method for Static Modulus of Elasticity and Poisson's Ratio of Concrete in Compression*; American Society for Testing and Materials: West Conshohocken, PA, USA, 2002.
56. Prachasaree, W.; Limkatanyu, S.; Hawa, A.; Samakrattakit, A. Samakrattakit. Development of equivalent stress block parameters for fly-ash based geopolymer concrete. *Arab J. Sci. Eng.* **2014**, *39*, 8549–8558. [[CrossRef](#)]
57. ACI 318. *Building Code Requirements for Structural Concrete and Commentary*; ACI Committee: Farmington Hills, MI, USA, 2014.
58. Thomas, R.; Peethamparan, S. Alkali-activated concrete: Engineering properties and stress-strain behaviour. *Constr. Build. Mater.* **2015**, *93*, 49–56. [[CrossRef](#)]
59. Wardhono, A. The durability of fly-ash geopolymer and alkali-activated slag concrete. Ph.D. Thesis, RMIT University, Melbourne, Australia, 2015.
60. Ng, T.; Foster, S. Development of high performance geopolymer concrete. In *Future in Mechanics and Structures and Materials*; Taylor&Francis: London, UK, 2008.
61. Diaz-Loya, E.I.; Allouche, E.N.; Vaidya, S. Mechanical properties of fly-ash based geopolymer concrete. *ACI Mater.* **2011**, *102*, 300–306.
62. Gunasekara, C.M. Influence of properties of fly ash from different sources on the mix design and performance of geopolymer concrete. Ph.D. Thesis, RMIT University, Melbourne, Australia, 2016.

63. Olivia, M.; Nikraz, H. Properties of fly-ash geopolymer concrete designed by Taguchi method. *Mater. Des.* **2012**, *36*, 191–198. [[CrossRef](#)]
64. C143/C143M. *Standard Test Method for Slump of Hydraulic-Cement Concrete*; American Society for Testing and Materials: West Conshohocken, PA, USA, 2015.
65. Junaid, M.T.; Kayali, O.; Khennane, A.; Black, J. A mix design procedure for low calcium alkali activated fly ash-based concretes. *Constr. Build. Mater.* **2015**, *79*, 301–310. [[CrossRef](#)]
66. Leung, C.K.Y. Concrete as a Building Material. In *Encyclopedia of Materials: Science and Technology*, 2nd ed.; Pergamon Press: Pergamon, Turkey, 2001; pp. 1471–1479. ISBN 978-0-08-043152-9.
67. Fang, G.; Ho, W.K.; Tu, W.; Zhang, M. Workability and mechanical properties of alkali-activated fly ash-slag concrete cured at ambient temperature. *Constr. Build. Mater.* **2018**, *172*, 476–487. [[CrossRef](#)]
68. Deb, P.S.; Nath, P.; Sarker, P.K. The effects of ground granulated blast-furnace slag blending with fly ash and activator content on the workability and strength properties of geopolymer concrete cured at ambient temperature. *Mater. Des.* **2014**, *62*, 32–39. [[CrossRef](#)]
69. Pangdaeng, S. Phoo-ngernkham, T.; Sata, V.; Chindaprasirt, P. Influence of curing conditions on properties of high calcium fly ash geopolymer containing Portland cement as additive. *Mater. Des.* **2014**, *53*, 269–275. [[CrossRef](#)]
70. Li, X.; Wang, Z.; Jiao, Z. Influence of Curing on the Strength Development of Calcium-Containing Geopolymer Mortar. *Materials* **2013**, *6*, 5069–5076. [[CrossRef](#)]
71. Abdollahnejad, Z.; Dalvand, A.; Mastali, M.; Luukkonen, T.; Illikainen, M. Luukkonen and M. Illikainen. Effects of waste ground glass and lime on the crystallinity and strength of geopolymers. *Mag. Concr. Res.* **2018**. [[CrossRef](#)]
72. Nazari, A.; Bagheri, A.; Riahi, S. Properties of geopolymer with seeded fly ash and rice husk barkash. *Mater. Sci. Eng.* **2011**, *24*, 73–95.
73. Das, B.; Neithalath, N. *Sustainable Construction and Building Materials*; Springer: Berlin/Heidelberg, Germany, 2018.
74. Vijai, K.; Kumutha, R.; Vishnuram, B.G. Effect of types of curing on strength of geopolymer concrete. *Int. J. Phys. Sci.* **2010**, *5*, 1419–1423.
75. Nath, P.; Sarker, P.K.; Rangan, V.B. Early age properties of low-calcium fly ash geopolymer concrete suitable for ambient curing. *Procedia Eng.* **2015**, *125*, 601–607. [[CrossRef](#)]
76. Dombrowski, K.; Buchwald, A.; Weil, M. The influence of calcium content on the structure and thermal performance of fly ash based geopolymers. *J. Mater. Sci.* **2007**, *42*, 3033–3043. [[CrossRef](#)]
77. Provis, J. Green concrete or red herring? —Future of alkali-activated materials. *Adv. Appl. Ceram.* **2014**, *113*, 472–477. [[CrossRef](#)]
78. Barbosa, V.F.; MacKenzie, K.J. Synthesis and thermal behavior of potassium sialate geopolymers. *Mater. Lett.* **2003**, *57*, 1477–1482. [[CrossRef](#)]
79. Lizcano, M.; Kim, H.S.; Basu, S.; Radovic, M. Mechanical properties of sodium and potassium activated metakaolin-based geopolymers. *J. Mater. Sci.* **2011**, *47*, 2607–2616. [[CrossRef](#)]
80. Hounsi, A.D.; Lecomte-Nana, G.; Djeteli, G.; Blanchart, P.; Alowanou, D.; Kpelou, P.; Napo, K.; Tchangbedji, G.; Praisler, M. How does Na, K alkali metal concentration change the early age structural characteristic of kaolin-based geopolymers. *Ceram. Int.* **2014**, *40*, 8593–8962. [[CrossRef](#)]
81. Committee, N.R. *In-place Strength Evaluation—A Recommended Practice*. NRMCA Publication 133; NRMCA: Silver Spring, MD, USA, 2003.
82. Pradip Nath, S.P. Use of OPC to improve setting and early strength properties of low calcium fly ash geopolymer concrete cured at room temperature. *Cem. Concr. Compos.* **2015**, *55*, 205–214. [[CrossRef](#)]
83. Hamidi, F.; Aslani, F.; Valizadeh, A. Compressive and tensile strength fracture models for heavyweight geopolymer concrete. *Eng. Fract. Mech.* **2020**, *231*, 107023. [[CrossRef](#)]
84. Abdollahnejad, Z.; Luukkonen, T.; Mastali, M.; Kinnunen, P.; Illikainen, M. Kinnunen and M. Illikainen. Development of One-Part Alkali-Activated Ceramic/Slag Binders Containing Recycled Ceramic Aggregates. *J. Civ. Eng.* **2019**, *31*. [[CrossRef](#)]
85. El-Newihy, A. Application of Impact Resonance Method for Evaluation of the Dynamic Elastic Properties of Polypropylene Fiber Reinforced Concrete. Ph.D. Dissertation, University of Victoria, Victoria, BC, Canada, 2017.

86. Massoud, S.; Deventer, J.v.; Mendis, P.; Lukey, G. Engineering properties of inorganic polymer concretes (IPCs). *Cem. Concr. Res.* **2007**, *37*, 251–257.
87. Fernandez-Jimenez, A.M.; Palomo, A.; Lopez-Hombrados, C. Lopez-Hombrados. Engineering properties of alkali-activated fly ash concrete. *ACI Mater. J.* **2006**, *103*, 106–112.
88. Duxson, P.S.W.M.; Mallicoat, S.W.; Lukey, G.C.; Kriven, W.M.; van Deventer, J.S. The effect of alkali and Si/Al ratio on the development of mechanical properties of metakaolin-based geopolymers. *Colloids Surfaces A Physicochem. Eng. Aspects* **2007**, *292*, 8–20. [[CrossRef](#)]
89. Sofi, M.; Van Deventer, J.S.J.; Mendis, P.A.; Lukey, G.C. Mendis and G. Lukey. Engineering properties of inorganic polymer concretes (IPCs). *Cem. Concr. Res.* **2007**, *37*, 251–257. [[CrossRef](#)]
90. Nath, P.; Sarker, P.K. Flexural strength and elastic modulus of ambient-cured blended low-calcium fly ash geopolymer concrete. *Constr. Build. Mater.* **2017**, *130*, 27–31. [[CrossRef](#)]
91. Granata, M.F.; Margiotta, P.; Arici, M. Simplified Procedure for Evaluating the Effects of Creep and Shrinkage on Prestressed Concrete Girder Bridges and the Application of European and North American Prediction Models. *J. Bridge Eng.* **2013**, *18*, 1281–1297. [[CrossRef](#)]
92. Argiz, C.; Sanjuán, M.Á.; Menéndez, E. Coal bottom ash for portland cement production. *Adv. Mater. Sci. Eng.* **2017**, *7*. [[CrossRef](#)]
93. Wongpa, J.; Kiattikomol, K.; Jaturapitakkul, C.; Chindaprasirt, P. Compressive strength, modulus of elasticity, and water permeability of inorganic polymer concrete. *Mater. Des.* **2010**, *31*, 4748–4775. [[CrossRef](#)]
94. Kar, A.; Halabe, U.B.; Ray, I.; Unnikrishnan, A. Nondestructive characterization of alkali activated fly ash and/or slag concrete. *Eur. Sci. J.* **2013**, *9*, 52–74.



© 2020 by the authors. Licensee MDPI, Basel, Switzerland. This article is an open access article distributed under the terms and conditions of the Creative Commons Attribution (CC BY) license (<http://creativecommons.org/licenses/by/4.0/>).